THE VISIBILITY OF TARGETS: DISCS VS GRATINGS

Gottar, L., Outtaleb, W., **Brémond, R**. & Tarel, J.-P.

Université Gustave Eiffel, Laboratoire CoSys, F-77440 Champs/Marne, France

roland.bremond@univ-eiffel.fr

Abstract

The CIE approach to target visibility is based on Blackwell's experimental data of contrast thresholds for uniform discs on uniform backgrounds. An analytical model of detection thresholds has been proposed by the CIE (1972; 1981) followed by Adrian (1989). Another line of research is based on the fact that the detection threshold of a periodic pattern can be derived from the detection thresholds of its Fourier components, using the Contrast Sensitivity Function (CSF) of the human eye. We use a computer vision algorithm to compare the two approaches: a bank of spatial filters is tuned in order to compute the visibility of edges in an image, in a way which is consistent with the CSF (Joulan et al., 2011a). It allows comparing the visibility computed from a CSF-based method to the visibility computed from Adrian's formula, on the same images.

Keywords: **Visibility, Contrast sensitivity function, detection threshold.**

1 Context

Understanding the visibility of contrasts has been among the first goals of the CIE, with the adoption of the Visibility curve V(λ) (Gibson, 1926) proposed by Gibson & Tyndall (1923). The investigation of contrast thresholds above which a target is visible made an important step ahead when Blackwell (1946) conducted an intensive study where millions of data were collected about the visibility of uniform discs on uniform backgrounds. These data formed the basis for the CIE approach of target visibility, leading to a model of target detection threshold taking many experimental factors into account (CIE, 1972; CIE, 1981). Following this line of reasoning, Adrian proposed a formula for the computation of the contrast threshold (Adrian, 1989).

Another line of research is based on the realization, in the 1960', that the visual system is nearly linear around threshold (Wandell, 1995). The detection threshold of a periodic visual pattern can be derived from the detection thresholds of its Fourier components (Campbell & Robson, 1968), using the contrast sensitivity function (CSF) of the human eye (Barten, 1999). This approach seems more general than modelling the detection of uniform targets, in the sense that any spatial pattern can be described by its Fourier components, while the psychophysical data accumulated on the visibility of uniform discs on uniform backgrounds cannot be easily generalized to other shapes (Crescenzo et al., 2018). However, this approach is restricted, at least in theory, to periodic patterns.

Surprisingly, these two approaches have not been compared so far to our knowledge, except by Joulan (2015). In this paper, we use the computer vision approach proposed par Joulan et al. (2011a), where a bank of spatial filters is tuned in order to compute the visibility of edges in an image, in a way which is consistent with the CSF approach. Computing the visibility of the edge of a uniform target on a uniform background with this image processing method allows comparing the visibility computed from a CSF-based method to the visibility computed from Adrian's formula, on the same images.

2 Previous work

2.1 Uniform target visibility

The visibility of a target can be computed from psychophysical data of the visibility of uniform discs on uniform backgrounds (Blackwell, 1946). This leads to a formula which fits most of the available data on such targets, as proposed by the CIE (1981) and by Adrian (1987; 1989) using the Visibility Level (VL) concept. The VL of a target is the ratio of its luminance contrast C_W over the contrast threshold C_{th} allowing 50% probability that the target is detected:

$$VL = \frac{C_W}{C_{th}} \tag{1}$$

where C_W denotes the Weber contrast:

$$C_W = \frac{L_t - L_b}{L_b}$$

with L_t the target luminance and L_b the background luminance. Adrian's model computes C_{th} as a function of the background luminance L_b, the apparent size α of the target, the target presentation time t, the contrast polarity and the viewer's age. The proposed formula is as follows:

$$\Delta L_{th} = \left(\frac{\phi^{1/2}}{\alpha} + {L_b}^{1/2}\right)^2 \cdot CP \cdot \left(\frac{a(L_b, \alpha) + t}{t}\right) \cdot AF \tag{2}$$

where ΔL_{th} is the luminance difference between object and background at detection threshold, CP is a contrast polarity factor (the contrast may be positive or negative), AF the Age Factor, while ϕ and a are functions associated to Ricco's law and Weber's law (see Adrian, 1989 for more details). From this equation, he computes the visibility level as:

$$VL = \frac{L_t - L_b}{\Delta L_{th}} \tag{3}$$

which is equivalent to Eq. 1.

2.2 Visibility of gratings

An alternative and more general method has been proposed, based on the Contrast Sensitivity Function (CSF) of the human eye. The CSF gives the contrast threshold C_{th} for sinusoidal gratings at any spatial frequency (the sensibility is the inverse of the contrast threshold). Considering gratings, the Michelson definition of contrast is used:

$$C_M = \frac{L_{\max} - L_{\min}}{L_{\max} + L_{\min}} \tag{4}$$

where L_{min} and L_{max} are respectively the minimal and maximal luminance in the pattern. The contrast sensitivity of a sine wave grating of spatial frequency f is the inverse of the contrast threshold:

$$\mathrm{CSF}(f) = \frac{1}{C_{th}(f)} \tag{5}$$

Campbell & Robson (1968) showed that the visibility of a periodic pattern can be described based on its Fourier components, considering that the contrast sensibility of each component is given by its CSF of the human eye for the corresponding spatial frequency. It is thus possible to estimate the visibility of any periodic pattern based on the CSF.

Various analytic models of the CSF have been proposed (e.g. Barten, 1999; Mantiuk et al., 2022), taking the background luminance and the angular size of the periodic pattern into account. In the following, we use Barten's simplified function (Barten, 1990), which is a good approximation in photopic vision:

$$\mathrm{CSF}(f) = afe^{-bf}\sqrt{1+ce^{bf}} \tag{6}$$

with

$$a = \frac{540\left(1+\frac{0.7}{L}\right)^{-0.2}}{\left(1+\frac{12}{w\left(1+\frac{f}{3}\right)}\right)^{2}};\ b = 0.3\left(1+\frac{100}{L}\right)^{0.15} \text{ and } c = 0.06$$

where *L* is the average luminance and *w* the stimulus size (see Fig. 1, left).

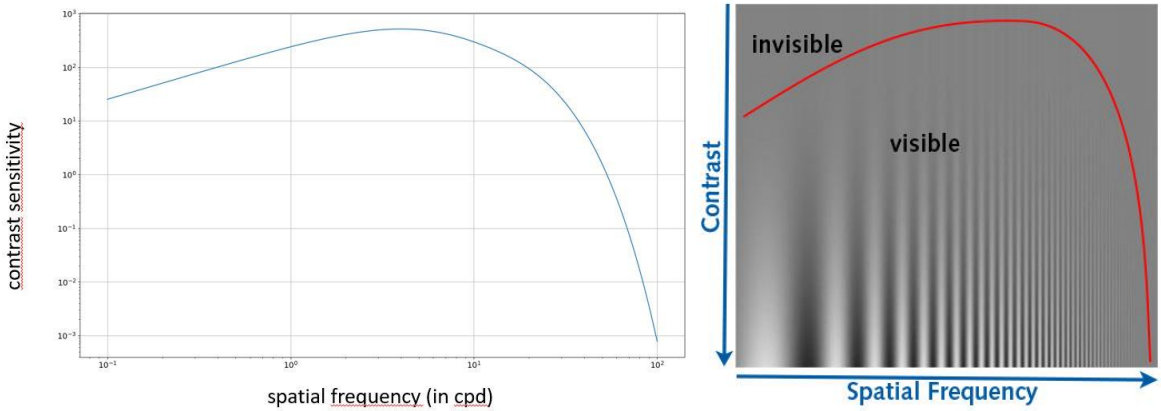

Figure 1: Left: Contrast Sensitivity Function after Barten (2004) with a background luminance L=100cd/m² and w=10°, see Eq. 6. Right: Contrast visibility for the human eye across spatial frequencies.

2.3 Edge Visibility

Joulan et al. (2011a, 2011b) proposed an image processing version of the CSF approach to compute the visibility of edges in an image. Firstly, a linear combination named SDoG, of Difference-of-Gausian (DoG) filters (see Fig. 2) is used to fit the CSF. Secondly, the visibility map is computed as the gradient norm of the image filtered by the 2D version of the SDoG, following Marr & Hildreth (1980) idea that the "strength" of an edge is proportional to the slope of the Laplacian at zero-crossings. Joulan's 2D DoG was given as:

$$DoG_{\sigma}(u,v) = \frac{1}{2\pi\sigma^2}\exp\left(-\frac{u^2+v^2}{2\sigma^2}\right) - \frac{1}{2\pi(\sigma\lambda)^2}\exp\left(-\frac{u^2+v^2}{2(\sigma\lambda)^2}\right) \tag{8}$$

where σ and σλ describe the spatial scales of the two Gaussians (Joulan uses λ=3 based on vision science data).

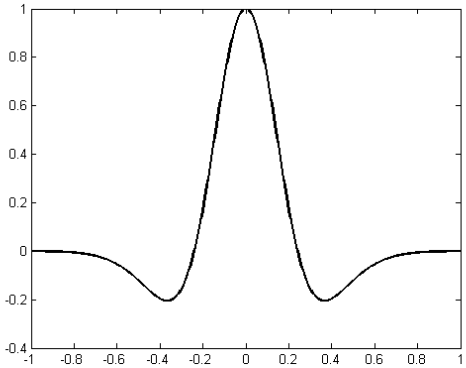

Figure 2: Example of a Difference of Gaussan filter in 1 dimension.

When applied to a 1D sine wave grating (see below Fig. 5a), this filter performs an amplitude modulation. Then, the value of σ which maximizes the amplitude of the filtered signal of spatial frequency f can be computed, leading to:

$$\sigma(\mathrm{f}) = \frac{1}{\pi f} \cdot \sqrt{\frac{\ln(\lambda)}{\lambda^2 - 1}} \tag{9}$$

Joulan et al. (2011a) followed Campbell & Robson's suggestion that the CSF results from a bank of pass-band filters. They used a linear combination of DoGs at various spatial scales, leading to a weighted SDoG filter (Sum of DoGs):

$$SDoG = \sum_1^n \omega_i DoG(f_i) \tag{10}$$

The SDoG is fitted on the CSF in such a way that, for several frequencies, the estimated visibility of a sine wave gratings with a given spatial frequency is equal to the CSF for this frequency. The full approach takes a CSF as input and computes an optimal bank of DoG filters in such a way that computing the SDoG is almost equivalent, in the spatial domain, to applying the CSF in the Fourier domain. The accuracy of the model depends on the number of DoGs in the SDoG, and any experimental CSF can be fitted, for instance the CSF including the observer's age as a parameter as in Joulan et al. (2015).

3 DoG model

The Joulan et al. (2011a, 2011b) original method has been improved in several ways as described in the following.

The CSF fitting algorithm, has been implemented in python based on a constrained minimization approach. It consists of optimizing a list of parameters: the weights ω_i and the frequencies f_i by minimizing an error function. In this computation, we use λ=3 as in Joulan et al. (2011a, 2011b), and Eq. 9 is used to compute the $\sigma(f_i)$ from the f_i. The Mean Absolute Error (MAE) is used as the error function, computing the mean of the absolute differences between the CSF and the reconstructed CSF on a set of uniformly sampled frequencies. To ensure that the model remains consistent with the functioning of the human visual system, we added two constraints:

- Each weight must be positive and large enough to contribute to the CSF; therefore, we ask that $\omega_i \geq 0.01$;
- Each frequency must lie within a range corresponding to visible objects, therefore, we ask that $0.01 \leq f_i \leq 100$ cycles per degree (cpd).

Table 1: frequencies and weights of the obtained DoGs.

	DoG_1	DoG_2	DoG_3	DoG_4	DoG_5	DoG_6
f_i	0.1502	0.4704	1.2017	2.6934	5.3886	10.3431
$\sigma(f_i)$	0.7855	0.2508	0.0982	0.0438	0.0219	0.0114
$\lambda\sigma(f_i)$	2.3566	0.7523	0.2945	0.1314	0.0657	0.0342
ω_i	46.8430	37.8333	32.0385	25.1881	7.9288	1.5160

With 6 DoGs, we obtained the values presented Table 1, also displayed Fig. 3 (left) in the frequency domain. The fit with Barten's CSF is very good between 0.5 cpd and 20 cpd, as shown in Fig. 3 (right), which includes the human peak of sensitivity around 3-4 cpd. In this

example, we used Barten's simplified CSF as the reference (Barten, 2004), but the proposed optimization also applies with another CSF curve.

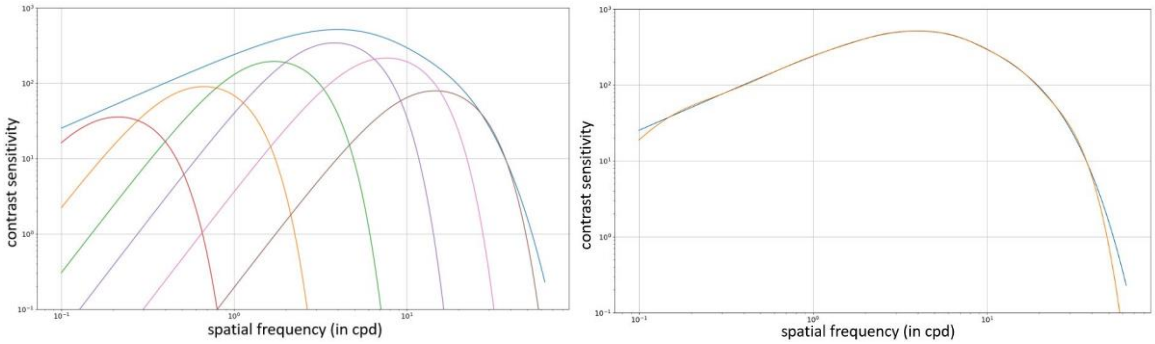

Figure 3. Left: DoGs 1 to 6 from table 1 plotted in the frequency domain, compared to Barten's CSF (in blue). Right: Comparison of Barten's CSF (in blue) and the SDoG (in orange).

Once the CSF fitting by the SDoG is obtained, the computation of the gradient norm on the image filtered using the SDoG leads to the so-called visibility map. To avoid border effect, the input image is assumed symmetrically replicated. Values in the visibility map being higher along edges, image edges are obtained by applying a non-maximum suppression algorithm (Canny, 1986) on the visibility map. As a result, the algorithm computes an edge visibility map where the detected edges of the image are valued with the visibility at each edge pixel. Finally, the edge visibility map is an image with zero outside edges, and the estimated visibility on edge pixels. Fig. 4 shows some examples of visibility images computed on natural images.

Figure 4: Examples of edge visibility maps computed with the proposed algorithm. Top: original images. Bottom: visibility maps.

Results

The algorithm was first tested on images of sinusoidal gratings of various spatial frequencies (Fig. 5, top), where the theoretical visibility can be computed from the CSF using Eq. 5: the sensitivity in the CSF is the inverse of the contrast threshold. The visibility of an edge is computed as the mean value of the visibility along this edge (in these images, the edge visibility is roughly constant along the edges). Fig. 6 (left) shows a very good fit between the visibility computed by image processing and the theoretical contrast sensitivity, for a large range of spatial frequencies (the similarity score is 99.72%). Moreover, we also checked whether a 2D version of these gratings, with circular sine waves (Fig. 7b), would lead to the same values of the edge visibility, and this is clearly the case (Fig. 6, right) with a similarity score of 99.74%.

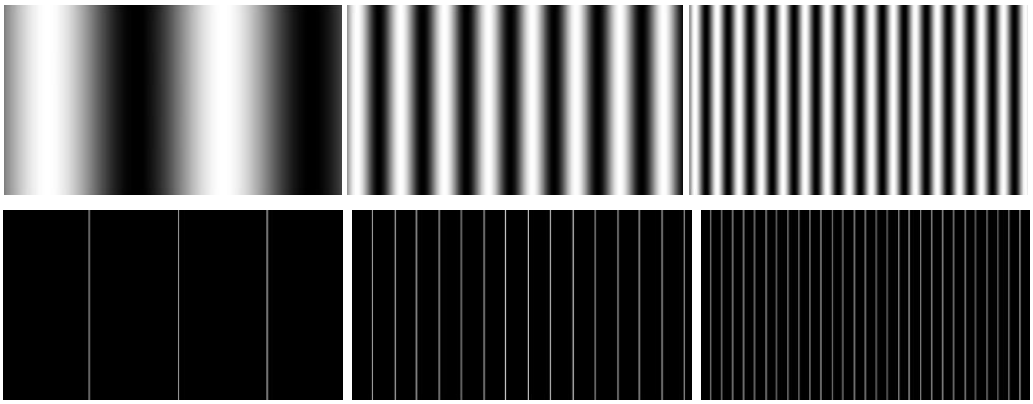

Figure 5: Top: images of sine wave gratings of various spatial frequencies. Bottom: images of the edges computed from the upper images.

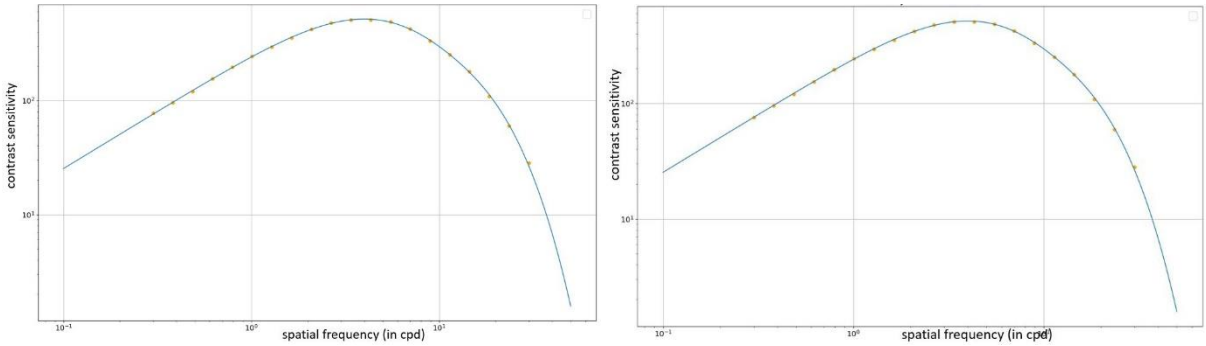

Figure 6: Contrast sensitivity according to Barten's CSF compared to the visibility of edges in images of 1D sine wave gratings as in Fig. 7a (left) and in images of 2D sine wave gratings as in Fig. 7b (Right).

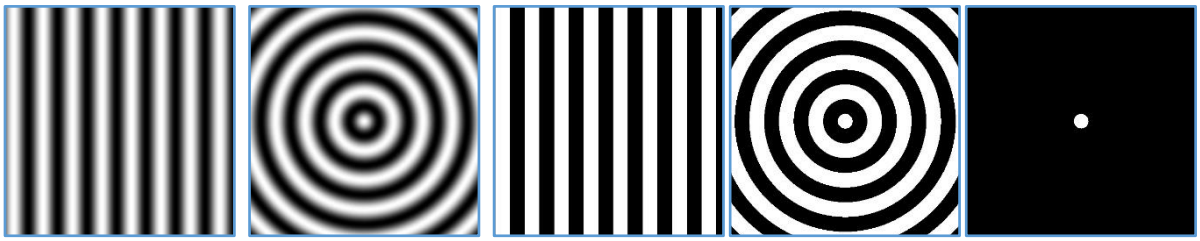

Figure 7: From left to right: (a) 1D sine wave grating, (b) 2D circular sine wave grating, (c) 1D square wave grating with the same spatial frequency, (d) 2D circular square wave grating, and (e) uniform target.

The SDoG model was then applied to a series of images with different properties (Fig. 7c-e). It was applied to square wave gratings either 1D or 2D (Fig. 2c & 2d), leading to the classical result of Campbell & Robson (1968) that the contrast sensitivity is proportional to that of sine wave gratings above 0.8 cpd, and nearly constant below. In the 1D case, this can be demonstrated from the decomposition of a periodic square grating as:

$$s(t) = \frac{4}{\pi} \sum_{k=1,3,5,\dots}^{\infty} \frac{1}{k} \, sin(2\,\pi k\, f\, t) \tag{10}$$

The visibility of this signal can be computed from the visibility of each of the sine waves, resulting in:

$$V(f) = \frac{4}{\pi} \sum_{k=1,3,5,\dots}^{\infty} \frac{1}{k} \, CSF(k\, f) \tag{11}$$

The visibility of square wave gratings is similar to the visibility of sine wave gratings for spatial frequencies above 1 cpd, and reaches a plateau below 1 cpd. Interestingly, this result also holds for 2D rings: the similarity score is 99.19% with the 1D square waves (Fig. 8, left), and 99.78% with the 2D square rings (Fig. 8, right).

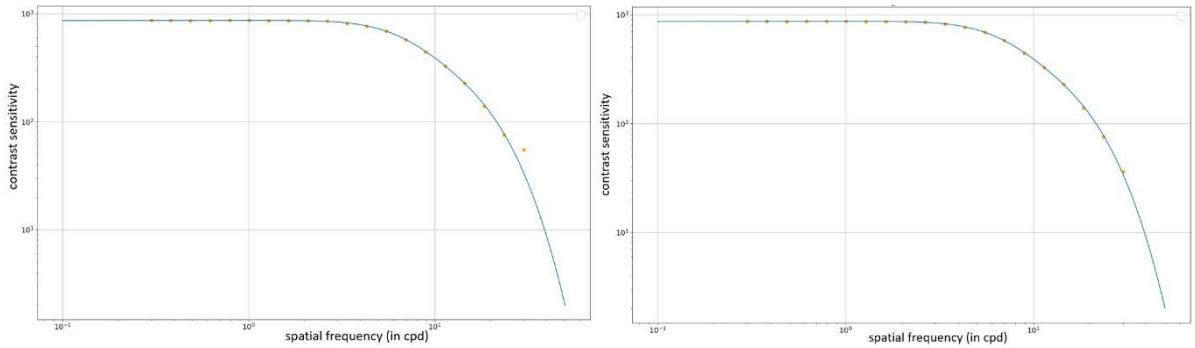

Figure 8: Left: Visibility of edges computed from 1D square waves of various spatial frequencies (see Fig. 7c), compared to the theoretical contrast sensitivity (Campbell & Robson, 1968). Right: same comparison with 2D circular square waves (Fig. 7d).

Finally, we used uniform discs (Fig. 7e) similar to the central disc in the 2D square wave images (compare Fig. 7d and 7e), but in an aperiodic image, in order to estimate the visibility of a single targets as in Blackwell's experiments (Blackwell, 1946; Adrian, 1989). Fig 9. Shows in continuous line the sensitivity of single targets (Adrian model, blue curve) and periodic square targets (CSF, orange curve). The main fact is that these two curves, however comparable in shape, are not equivalent, and a visibility cannot be on the two curves at the same time.

The blue and orange spots in Fig. 9 represent the visibility of 2D square waves (orange) for various spatial frequencies (Fig 7d) and the visibility of single targets of the same size as the central disc in the square waves (Fig. 7e), computed with our image processing model with a background of 100 cd/m^2. The blue and orange spots are very near to each other, meaning that the computed visibility of the single target is quite close to the visibility of the same target when surrounded by concentric rings as in Fig. 7d. In short, the proposed model, simulating human vision based on a CSF, does not allow to quantitatively estimate the visibility of single targets as proposed by Adrian (1987; 1989).

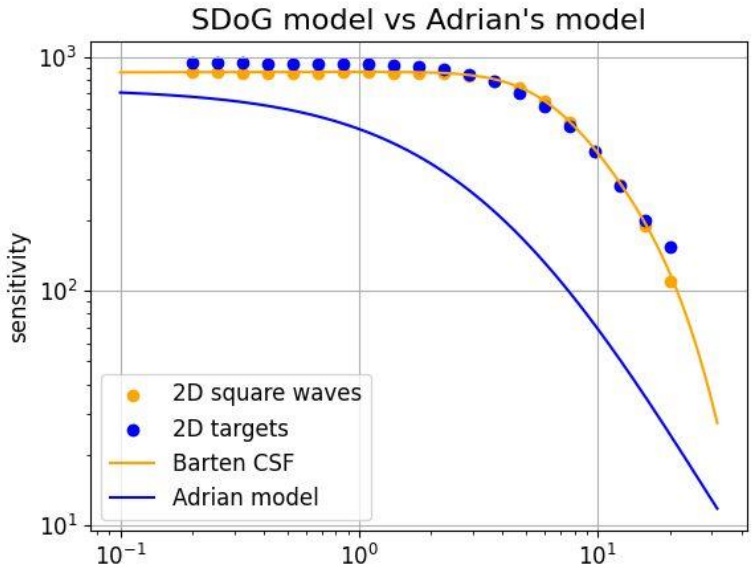

Figure 9: Theoretical and computed visibility for targets of various shapes and sizes.

To understand this difference, it is worth noting that Barten's simplified CSF, which was considered here in order to tune the SDoG filter, may be different from the actual CSF of the participants of Blackwell's and Adrian's experiments, leading to possible discrepancies. The differences between the computed visibility of a uniform disc and a periodic pattern should also be discussed in view of a quantitative comparison that could be done step by step, in order to understand the limits of each of these models. In our case, given that the CSF applies to periodic stimuli, other types of periodic targets may be investigated, for a better understanding of the influence of the rings around the central target on the visibility of this central target.

4 Conclusion

The results obtained with our operator, fitted on Barten's CSF, proved quite satisfactory. The 1D and 2D gratings (bars and rings) have almost exactly the same visibility (*waves* vs *circles* in Fig. 7), which is a good point for the CSF-based model and should help understanding the relation between the visibility of 1D gratings and the visibility of uniform 2D targets. Also, the proposed model is consistent with Cambell & Robson (1968) regarding the visibility of square gratings, either 1D or 2D.

However, when we compared our results to Adrian's model of the visibility of uniform discs, we found a discrepancy between the two, consistent with other limitations of image processing algorithms when it comes to simulate human vision (Cai et al., 2025). Among the possible explanations for the discrepancy between the visibility computed by our model for periodic and aperiodic targets, the following are worth investigating:

- The definition of visibility and contrast: Blackwell and the CSF do not use the same definition for the contrast (Weber vs Michelson), which may explain that the visibility thresholds differ.

- Adrian's formula includes more parameters than Barten's CSF (e.g. observer's age, target presentation time). Barten's CSF does not use these parameters, so we assumed it was based on ideal conditions (minimum age and maximum exposure time). The ongoing work of CIE reportership DR 1-73 on "*Modelling contrast sensitivity functions across a large parameter space*" may help investigating this aspect in future work.

References

ADRIAN, W. 1989, Visibility of Targets: Model for Calculation, *Lighting Research and Technology*, 21(4), 181-188.

BARTEN, P. 1990. *Evaluation of subjective image quality with the square-root integral method. Journal of the Optical Society of America A, 7, 2024-2031.*

BARTEN, P. 1999. *Contrast sensitivity of the human eye*. SPIE, Bellingham, WA.

BLACKWELL, H. R. 1946. Contrast thresholds of the human eye. *Journal of the Optical Society of America*, 36(11), 624-643.

CAI, Y., YIN, F., HAMMOU, D. & MANTIUK, R. (2025). Do computer vision foundation models learn the low-level characteristics of the human visual system? To appear in Proc. CVPR, Nashville, TS. https://arxiv.org/abs/2502.20256

CAMPBELL, F. W., and ROBSON, J. G. 1968. Application of Fourier analysis to the visibility of gratings. *Journal of Physiology*, 197 (3), 551-566.

CANNY, J. (1986). A Computational Approach to Edge Detection. *IEEE Transactions on Pattern Analysis and Machine Intelligence* 8(6), 679-698.

CIE. 1981. CIE 19/2.1:1981. *An analytical model for describing the influence of lighting parameters upon visual performance. Volume 1: Technical foundations*. Vienna: CIE.

GIBSON, K. S. (1926). *The relative visibility function*. Sixth session of the CIE (July 1924), Genève. Recueil des travaux et compte rendus des séances, pp. 232–238, Cambridge University Press.

GIBSON, K. S. and TYNDALL, E. (1923). *Visibility of radiant energy*. Technical report, Bureau of Standards, Wahington DC.

HALMAOUI, H., JOULAN, K., HAUTIERE, N., CORD, A. and BREMOND, R. (2015). A Quantitative Model of the Driver's Reaction Time in Daytime Fog. Application to a HUD-based ADAS. *IET Intelligent Transport Systems* 9(4):375-381.

JOULAN (2015). *Estimation de la visibilité routière du point de vue du conducteur : contribution aux aides à la conduite*. PhD dissertation, Université Gustave Eiffel, Paris, France.

JOULAN, K., HAUTIERE, N. and BREMOND, R. (2011a). *A Unified CSF-based Framework for Edge Detection and Edge Visibility*. In proc. CVPR workshop on biologically-consistent vision, Colorado Springs, CO, USA.

JOULAN, K., HAUTIERE, N. and BREMOND, R. (2011b). *Contrast Sensitivity Functions for Road Visibility Estimation*. In Proc. 27th session of the Commission Internationale de l'Eclairage, Sun City, South Africa.

JOULAN, K., HAUTIERE, N. and BREMOND, R. (2015). Towards an Analytical Age-dependent Model of Contrast Sensitivity Functions for an Ageing Society. *The Scientific World Journal* 625034:1-11.

MANTIUK, R. K., ASHRAF, M. and CHAPIRO, A. 2022. StelaCSF, a unified model of contrast sensitivity as the function of spatio-temporal frequency, eccentricity, luminance and area. *ACM Transactions on Graphics* 41(4), 145.

MARR, D. and HILDRETH, E. (1980). Theory of edge detection. *Proceedings of the Royal Society B* 207, 187-217.

WANDELL, B. (1995). *Foundations of vision*. Oxford University Press, Oxford, UK.